Journal of Power Sources 196 (2011) 10141–10147

Contents lists available at ScienceDirect

Journal of Power Sources

journal homepage: www.elsevier.com/locate/jpowsour

Capacity-fading prediction of lithium-ion batteries based on discharge curves analysis

Kohei Honkura [a,*], Ko Takahashi [a], Tatsuo Horiba [b]

[a] Hitachi Ltd., Hitachi Research Laboratory, 1-1, Omika-cho 7-chome, Hitachi, Ibaraki 319-1292, Japan
[b] Shin-Kobe Electric Machinery Co., Ltd., 2200, Fukaya, Saitama 369-0297, Japan

ARTICLE INFO

Article history:
Received 20 May 2011
Received in revised form 3 August 2011
Accepted 4 August 2011
Available online 10 August 2011

Keywords:
Lithium ion batteries
Discharge curve analysis
Capacity fading
Life prediction

ABSTRACT

We have developed a new technology to predict capacity fading of lithium-ion cells using the analysis of their discharge curves. A cell capacity is deduced from the cell voltage window and the cell discharge curve, which was obtained by superimposing discharge curves of the positive and negative electrodes. This new technology consists of three steps: first, to analyze cell discharge curves measured during the calendar life test in order to evaluate deterioration indicators such as the positive and negative usable capacities and the irreversible capacities caused by the side reactions; secondly, to formulate these indicators as the functions of the test time; lastly, to produce the cell discharge curves by using these functions and deduce corresponding cell capacity, over storage days for prediction.

Prediction of the faded capacities of the cells after a 960 day calendar life test was attempted with the data up to 360 days using the technology described above and the conventional method by extrapolating capacity-fading data in accordance with square-root time rule. Consequently, the proposed technology predicted the faded capacities more precisely than the conventional method, particularly under severe conditions.

1. Introduction

The emerging introduction of large-sized lithium-ion batteries into various applications makes the technology that can predict their lifetime much more important than before. The battery life is usually evaluated by extrapolating the capacity-fading data of calendar life tests or cycle life tests. The extrapolation method is based on the assumption that the capacity fading is proportional to the square root of time, which is called $t^{1/2}$ rule [1–4].

The $t^{1/2}$ rule was proposed by Peled as a mathematical model for the formation and growth of solid electrolyte interphase (SEI) [1]. SEI is formed by the side reactions between intercalated lithium ions and the electrolyte at the negative electrode surface and consumes available lithium ions. Therefore, SEI growth is directly related to the capacity fading, and the $t^{1/2}$ rule has been applied to the capacity fading of batteries. However, capacity-fading predictions made by using the $t^{1/2}$ rule were not always consistent with actual data, especially in long term or severe tests.

The inconsistency between the predicted and actual capacity fading seemed to be derived from the assumption that capacity fading was simply caused by SEI formation, neglecting the effects of other factors. Ramadass et al. proposed to divide the capacity fading of the lithium-ion cells into the rate capability loss, the active material loss and the lithium-ion loss through disassembling the deteriorated lithium-ion cells [5]. Though this method enabled us to decide active material losses directly, we could not observe the continuous deterioration of active material losses.

Bloom et al. developed non-destructive "differential voltage analysis" using the relation between capacity (Q) and differential voltage (dV/dQ) [6]. The "differential voltage analysis" has the potential to precisely separate the discharge curves of the cells into the discharge curves of the positive and negative electrodes, though Bloom et al. have not made use of it.

Zhang and White analyzed the discharge curves of lithium-ion cells through single particle model simulation and evaluate the usable positive and negative active materials [7]. Recently, Smith et al. have shown the "differential capacity analysis", which studies discharge curves of dQ/dV vs. V [8]. Both groups analyzed discharge curves of the cells and proposed two kinds of deterioration indicators: the positive and negative active material masses and their electrode potentials. But both groups have not determined the quantitative relationship between these indicators. Thus, their analysis results have not been applied to the capacity fading predictions by now.

We have developed a mathematically arranged "differential voltage analysis" technology with which we can separate visually the discharge curves of lithium-ion cells into those of the positive and negative electrodes. In the process of separation, two kinds

* Corresponding author. Tel.: +81 294 52 5111; fax: +81 294 52 7636.
E-mail address: kohei.honkura.tt@hitachi.com (K. Honkura).

0378-7753/$ – see front matter © 2011 Elsevier B.V. All rights reserved.
doi:10.1016/j.jpowsour.2011.08.020

of deterioration indicators, already proposed in previous works as shown above [7,8], were quantitatively evaluated. Furthermore, we derived the irreversible lithium-ion loss consumed in SEI growth from the results of curve analysis [9]. We treated three basic deterioration indicators, irreversible capacity, and the usable positive and negative active material losses, assuming to be independent each other. Since this analysis is non-destructive, we can trace the changes of these indicators during the calendar life or cycle life tests. In this work, we applied this analysis to the calendar life test results of lithium-ion cells and predicted the discharge curves and capacities of the cells.

2. Experimental

2.1. Calendar life tests

We fabricated 0.7 Ah class 18,650-type cylindrical cells and used them to measure discharge curves during calendar life tests. The active materials of the cells were a manganese-based layered-structure oxide for the positive electrode and a hard carbon for the negative electrode. The positive electrode contained 7.13 g of active materials, while the negative contained 3.22 g. The positive and negative electrodes were formed on the both side of aluminum and copper foils by ordinary slurry coating process. Both of the finished electrodes were wound together with separators and sealed into a cylindrical can with the electrolyte of 1 mol L^{-1} lithium hexafluorophosphate in a mixture of organic carbonates.

The initial discharge curve and initial discharge capacities for the cells were measured between 4.1 and 2.7 V at 24 mA, which was regarded as small current enough to obtain sufficient capacity of the cell, after initial conditioning. The average initial capacity of them was 0.70 Ah and it was used as the rated capacity by which C rate was defined during the whole span of the calendar life test. Then the cells were charged up to 3.63 V which is the midpoint of the cell discharge curve, and then stored at 25 °C or 60 °C. After 30 days of storage, they were discharged, charged, and discharged at less than C/25 at 25 °C to measure the discharge curves and capacities (charge–discharge test). They were then charged up to 3.63 V at 1 C rate in CC/CV mode and stored again at each specific temperature. The test interval was changed from 30 days at the initial stage to 60 days after 450 days. This procedure was repeated until 960 days of storage so as to prove the validity of our capacity-fading prediction technology.

2.2. Half-cell test

We measured half-cell discharge curves of the positive and negative electrodes at fresh state to use them for reproducing the discharge curves of the single cells. These half cells consisted of a pristine positive or negative electrode of 1.8 cm^2, which were small pieces of the electrodes with the same specifications for 18,650 test cells, as the working electrode, a separator, an electrolyte, and a lithium foil as the counter and reference electrodes. They were assembled in an argon glove box at room temperature. Then we charged and discharged them at 0.1 mA (about C/50 rate) between 3.0 and 4.3 V for the positive half cell and between 0.005 and 1.5 V for the negative half cell.

Battery testing system, TOSCAT-3000, Toyo System Co., was used for charge–discharge tests of 18,650 cells and half cells.

3. State analysis

3.1. Discharge curve fitting

The following sentences contain many alphabetical symbols with and without suffixes. Please consult the "List of symbols" summarizing their precise definitions at the end of this paper when necessary.

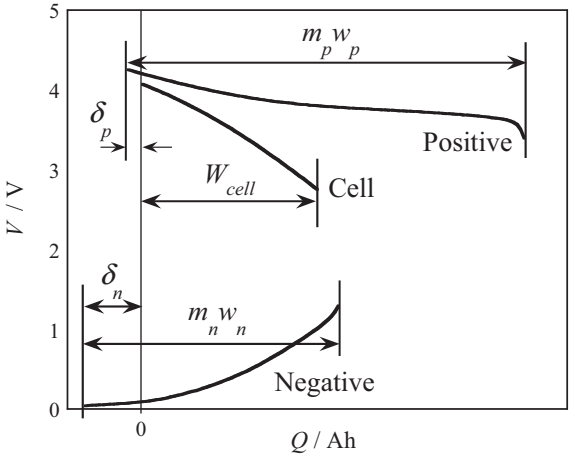

Fig. 1. Relationship among discharge curves and related parameters.

The cell voltage V_{cell} (V) is the difference between the positive electrode potential V_p (V) and the negative electrode potential V_n (V). Since V_{cell} depends on the discharged capacity Q (Ah), the discharge curves of Q–V_{cell}, Q–V_p, and Q–V_n will be the functions of $V_{cell}(Q)$, $V_p(Q)$, and $V_n(Q)$, respectively. Note that Q is not full capacity of cell W_{cell} (Ah), but is discharged quantity of electricity and can be obtained by just multiplying discharge current by discharge time. Supposing discharge current is small enough, we can neglect the voltage drop due to the internal resistance of the cell, and the $V_{cell}(Q)$ will be represented as follows:

$$V_{cell}(Q) = V_p(Q) - V_n(Q). \tag{1}$$

$V_p(Q)$ and $V_n(Q)$ were transformed into the specific discharge curves of the positive and negative electrodes denoted as $V_{sp,p}(q_p)$ and $V_{sp,n}(q_n)$, where q (Ah g^{-1}) was the discharged capacity per unit mass of the active material and V_{sp} (V) denoted the electrode potential. The relationship of q_p and q_n to Q is represented in Eq. (2) with the help of other parameters:

$$Q = m_p q_p - \delta_p = m_n q_n - \delta_n, \tag{2}$$

where m_p and m_n (g) are the usable masses of positive and negative active materials defined as the masses involved in the discharge reactions and contributing to the discharge capacity. δ_p and δ_n (Ah) can be regarded as constant if the following two conditions are satisfied during discharging to measure $V_{cell}(Q)$: (1) m_p and m_n do not change, and (2) q_p and q_n are varied not by irreversible side reactions that cause $m_p \Delta q_p$ and $m_n \Delta q_n$ to differ, but by reversible charge–discharge reactions in which $m_p \Delta q_p$ are equal to $m_n \Delta q_n$.

Fig. 1 illustrates the relationship among discharge curves and related parameters described above. W_{cell} is the full capacity of the cell defined in accordance with its own charge–discharge conditions. w_p and w_n represent the full capacities per unit mass of the positive and negative active materials, which are defined in accordance with the capacities observed for the potential ranges mentioned in Section 2.2. They are not variables but constants, differing from q_p and q_n. Thus, $m_p w_p$ and $m_n w_n$ are full capacities of the positive and the negative electrodes in the cell. δ_p and δ_n are the marginal capacities, which remain uncharged even after the lithium-ion cell are charged to the upper limit of the cell voltage. We can also regard them as the capacities that are still discharged even if the cell is in fully charged state, $Q = 0$.

Applying Eq. (2) to Eq. (1) transforms $V_p(Q)$ and $V_n(Q)$ into $V_{sp,p}(q_p)$ and $V_{sp,n}(q_n)$. Then, Eq. (1) will be

$$V_{cell}(Q) = V_{sp,p}(q_p) - V_{sp,n}(q_n). \tag{3}$$

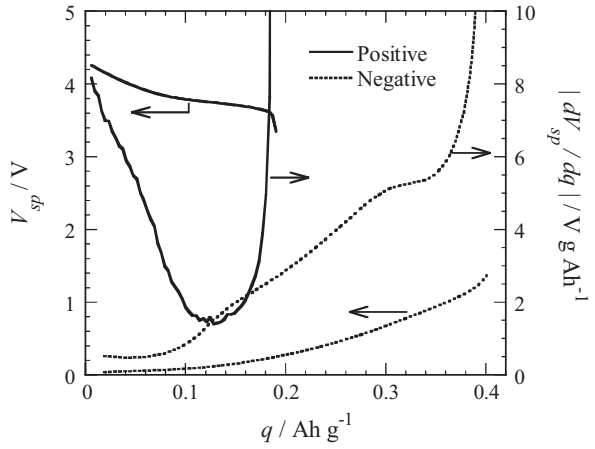

Fig. 2. Specific discharge curves of positive and negative electrodes and their differential forms measured with half cells.

Supposing $V_{sp,p}(q_p)$ and $V_{sp,n}(q_n)$ are specified, measured discharge curves of the cells $V_{cell}(Q)$ can be reproduced using Eqs. (2) and (3) by adjusting m_p, m_n, δ_p, and δ_n as free parameters. Fig. 2 shows examples of $V_{sp,p}(q_p)$ and $V_{sp,n}(q_n)$ and their differential form $dV_{sp,p}(q_p)/dq_p$ and $dV_{sp,n}(q_n)/dq_n$ measured with a half cell.

The reason why $V_{sp}(q)$ are transformed into the differential form is as follows. Fitting of m_p, m_n, δ_p, and δ_n in Eqs. (2) and (3) sometimes resulted in plural candidates that were equally accurate. Q–V discharge curves of the cells have flexibility and uncertainty to be fitted well with wrong parameters due to their simple and monotonous shapes. If we differentiate both sides of Eq. (3) with respect to Q and then replace dQ with $m_p dq_p$ and $m_n dq_n$ on the basis of Eq. (2), the differential discharge curves $dV_{cell}(Q)/dQ$ will be

$$\frac{dV_{cell}(Q)}{dQ} = \frac{dV_p(Q)}{dQ} - \frac{dV_n(Q)}{dQ} = \frac{1}{m_p}\frac{dV_{sp,p}(q_p)}{dq_p} - \frac{1}{m_n}\frac{dV_{sp,n}(q_n)}{dq_n}. \quad (4)$$

When the differential specific discharge curves of the positive and the negative electrodes, $dV_{sp,p}(q_p)/dq_p$ and $dV_{sp,n}(q_n)/dq_n$, are specified, the measured differential discharge curves of the cells, $dV_{cell}(Q)/dQ$, can be reproduced by Eqs. (2) and (4), like the case of Q–V discharge curves shown as Eq. (3). $dV_{sp,p}(q_p)/dq_p$ and $dV_{sp,n}(q_n)/dq_n$ have the shapes with amplified variation, peaks, and shoulders as shown in Fig. 2; the values of differential cell voltage dV_{cell}/dQ amplify as m_p and m_n decrease in accordance with Eq. (4). These features provide us with the clues to distinguish the most reliable fitting result among some candidates. Therefore, we can fit $dV_{cell}(Q)/dQ$ with suitable m_p, m_n, δ_p, and δ_n properly.

3.2. Deriving the irreversible lithium-ion loss (Li_{loss})

The capacity of irreversible lithium-ion loss caused by the side reactions, Li_{loss}, was estimated using the reproduced discharge curves of the cells. The lithium-ion cells were usually stored at specific temperatures and periodically cycled at 25 °C during the calendar life test. We supposed that the side reactions consuming lithium ions to form SEI were caused not by the charge–discharge test but by the self discharge during storage.

When self discharge happens, some lithium ions come out of the negative active material while some other lithium ions in the electrolyte go into the positive active material. The flow rate of lithium ions from the negative electrode is $m_n(dq_n/dt)$ (Ah day^{-1}), where t is the days for which the lithium-ion cells was stored at a specific temperature. Similarly the flow rate of lithium ions into the positive active material is $m_p(dq_p/dt)$. $m_n(dq_n/dt)$ is equal to $m_p(dq_p/dt)$ in reversible reactions, while $m_n(dq_n/dt)$ is larger than $m_p(dq_p/dt)$ in irreversible reactions due to the trapped lithium ions in SEI. Since we assumed $m_p(dq_p/dt)$ as the reversible self discharge rate, $[m_n(dq_n/dt) - m_p(dq_p/dt)]$ corresponds to the irreversible self discharge rate. Consequently, the irreversible lithium-ion loss during storage from t_1 to t_2, ΔLi_{loss} (Ah), will be

$$\Delta Li_{loss} = \int_{t_1}^{t_2} \left(m_n \frac{dq_n}{dt} - m_p \frac{dq_p}{dt} \right) dt. \quad (5)$$

Although the integral is difficult to do in actual cases because of the unknown functions $m(t)$ and $q(t)$, we can calculate it if the decrease rate of m is low. When this is the case, replacing the function $m(t)$ with the intermediate value $[m(t_1)+m(t_2)]/2$ barely affects the result. Hence we evaluated the increment of irreversible lithium loss ΔLi_{loss} from t_1 to t_2 by

$$\Delta Li_{loss} \cong \frac{m_n(t_1)+m_n(t_2)}{2}[q_n(t_2)-q_n(t_1)] - \frac{m_p(t_1)+m_p(t_2)}{2}[q_p(t_2)-q_p(t_1)]. \quad (6)$$

The usable masses of active materials just before and after storage, $m(t_1)$ and $m(t_2)$, were evaluated by fitting $dV_{cell}(Q)/dQ$ measured at t_1 and t_2. The discharged capacities per unit mass of active material at t_1 and t_2, $q(t_1)$ and $q(t_2)$, were evaluated in accordance with the following five steps: (1) record the open circuit voltages (OCVs) of the cell at t_1 and t_2; (2) reproduce $dV_{cell}(Q)/dQ$ measured at t_1 and t_2 by fitting; (3) transform the fitting result of Q–dV/dQ discharge curves, i.e. $dV_{cell}(Q)/dQ$, $dV_p(Q)/dQ$, $dV_n(Q)/dQ$, into Q–V discharge curves, i.e. $V_{cell}(Q)$, $V_p(Q)$, and $V_n(Q)$; (4) estimate V_p and V_n corresponding to OCVs using the transformed fitting results; and (5) derive q_p and q_n corresponding to V_p and V_n from the specific curves for $V = V_{sp}(q)$.

4. Results and discussion

4.1. Half cell test and calendar life test results

The specific discharge curves and specific differential discharge curves such as those shown in Fig. 2 were measured by a half-cell test. Capacity changes in lithium-ion cells during the calendar life test are shown in Fig. 3. The horizontal axis is the square root of the storage days at the specific temperatures. As shown in Fig. 3, the

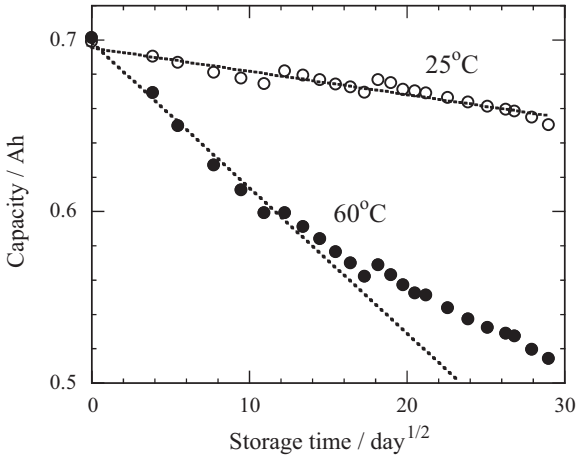

Fig. 3. Capacity changes of lithium-ion cells in calendar life test at 25 °C or 60 °C at 3.63 V.

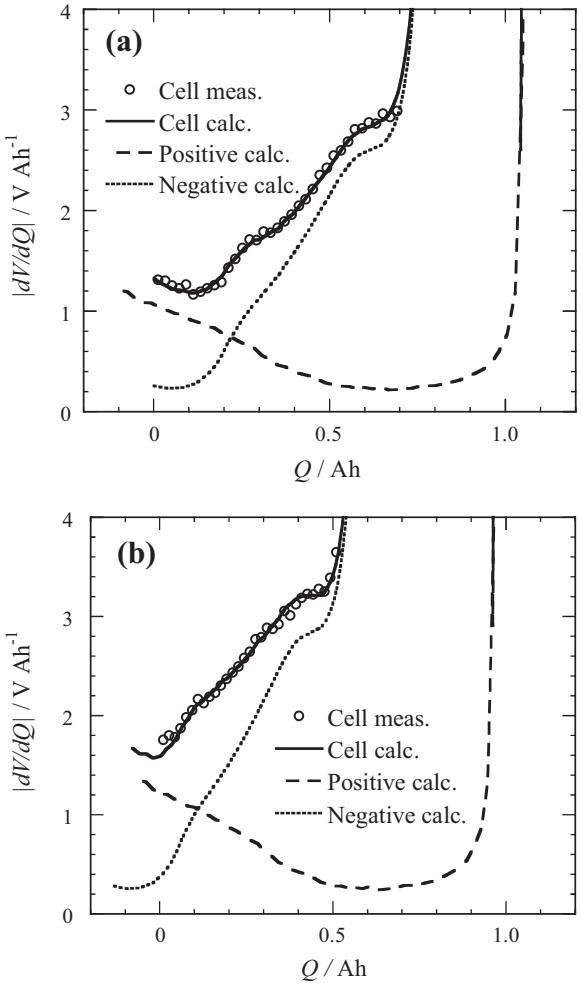

Fig. 4. Fitting results of differential discharge curves of lithium-ion cells: (a) in initial state, and (b) stored at 60 °C for 720 days.

change in the capacity at 25 °C followed the $t^{1/2}$ rule represented by the dotted line, while that at 60 °C gradually deviated from the $t^{1/2}$ rule.

We applied the state analysis we developed to elucidate the reason for this difference. Fig. 4 shows the fitting results of the differential discharge curves of the cell, $dV_{cell}(Q)/dQ$ along with $dV_p(Q)/dQ$ and $dV_n(Q)/dQ$, measured at 25 °C: Fig. 4a before storage and Fig. 4b after storage at 60 °C for 720 days. Both differential discharge curves of the cell were fitted to the measured data very well. Fig. 4a contains the effect of irreversible capacities caused by side reactions in the very first charge, which is reflected to the large horizontal gap between the end of the discharge curve of the positive and negative electrode. When a side reaction occurs at the negative electrode and consumes lithium ions coming from the positive electrode during the first charge, the potential of the negative electrode remains unchanged, while the potential of the positive electrode rises. Hence, the potential difference between the positive and negative electrode changes, which slides $dV_p(Q)/dQ$ and $dV_n(Q)/dQ$ in opposite direction horizontally to make the gap between them larger. Comparing $dV_{cell}(Q)/dQ$ after 720 days in Fig. 4(b) with that before storage in Fig. 4(a), the whole $dV_{cell}(Q)/dQ$ shifted upward while the horizontal width shrunk, i.e. the differential voltage dV/dQ values increased as the cell capacity decreased from 0.69 Ah to 0.52 Ah. The upward shift is caused mainly by decrease of the usable masses of the positive and negative active materials, m_p and m_n. The evaluated m_p and m_n were 6.45 g and 2.02 g in the initial state,

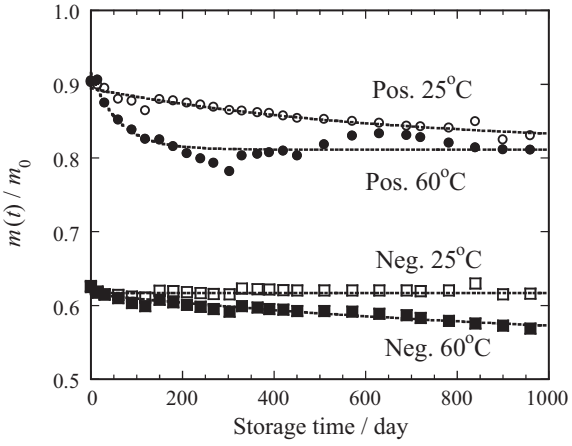

Fig. 5. Utilization ratios of active materials in positive and negative electrodes.

which decreased to 5.77 g and 1.86 g after 720 day storage. As m_p and m_n decreased, differential potential of the positive and negative electrodes, dV_p/dQ and dV_n/dQ, increased as shown in Eq. (4). Hence, positive and negative discharge curves also shifted upward. The horizontal position of $dV_p(Q)/dQ$ against $dV_n(Q)/dQ$ changed, e.g. $\delta_p > \delta_n$ at the initial, while $\delta_n > \delta_p$ after 720 days. This change is presumed to be caused by the side reactions at the surface of the negative active material [6]. When a side reaction occurs at the negative electrode during storage, the intercalated lithium ions are consumed and the potential of the negative electrode rises, while the potential of the positive electrode remains unchanged. It also results in increase of the horizontal gap between $dV_p(Q)/dQ$ and $dV_n(Q)/dQ$. All the measured $dV_{cell}(Q)/dQ$ in the calendar life tests were well fitted in the same way as shown in Fig. 4. During the fitting, every $dV_{cell}(Q)/dQ$ was consequently resolved into the four parameters, m_p, m_n, δ_p, and δ_n, which enabled us to reproduce the original $dV_{cell}(Q)/dQ$.

Fig. 5 plots the calculated utilization ratios of active materials $m(t)/m_0$, which are the ratios of the mass of usable active materials to the mounted. The utilization ratios of both the positive and negative electrodes decreased exponentially over the test time. The respective dotted lines are the fitting curves formulated as follows

$$\frac{m(t)}{m_0} = \alpha - \beta(1 - e^{-t/\tau}) \tag{7}$$

where $m(t)$ is usable mass of the active material as a function of the storage time t, m_0 is the mounted mass of the active material on the positive or negative electrode, α is the initial utilization ratio, β is the coefficient of extent of the decreasing utilization ratio, and τ is the time constant of the fading process. The calculated values of the fitting constants in Eq. (7) are shown in Table 1. β at 60 °C was larger than that at 25 °C, and τ at 60 °C was smaller than that at 25 °C. This implies that the usable active materials fade rapidly at high temperatures. The difference of positive electrode β between at 60 °C and at 25 °C is small, while τ at 60 °C is around one tenth of that at 25 °C. This is consistent with the quick decrease of $m(t)/m_0$ with time at higher temperatures, for smaller τ corresponds to quick decrease of $m(t)/m_0$. β for negative electrode at 25 °C is a negative value, which means that $m(t)/m_0$ did not decrease but increased as

Table 1
Parameters for usable masses decreasing in positive and negative electrodes.

Electrode	m_0/g	T/°C	α	β	τ/day
Positive	7.13	25	0.8941	0.0773	633.8
		60	0.9147	0.1036	61.1
Negative	3.22	25	0.6170	−0.0013	9.08×10^5
		60	0.6155	0.0745	1163.5

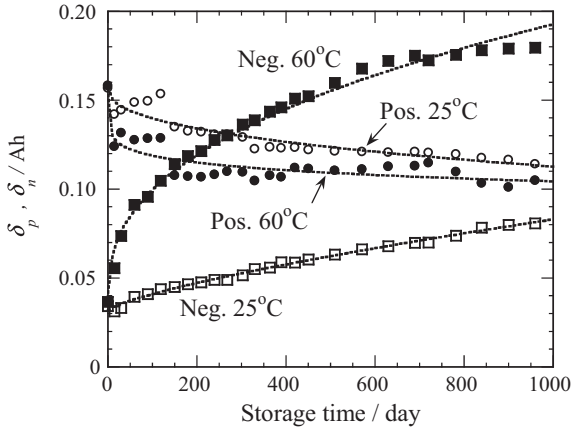

Fig. 6. Marginal capacities of the positive and negative electrode.

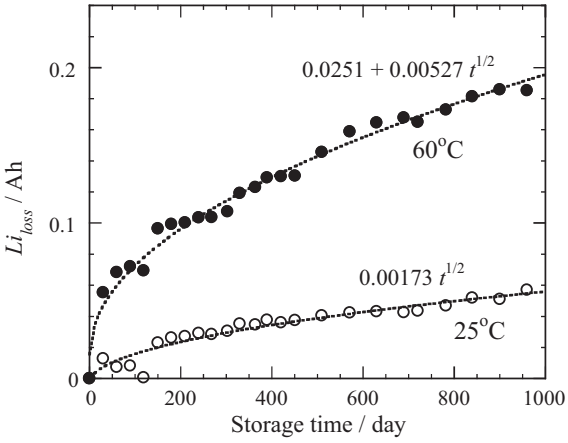

Fig. 8. Accumulated irreversible capacity losses by side reactions.

time passed. Therefore, the curve fitting for the negative electrode at 25 °C contained some errors caused by the unchanged values and measurement errors. As for the negative electrode, τ at 25 °C is one thousand times as large as that at 60 °C. This result is consistent with almost unchanged $m(t)/m_0$ for the negative electrode at 25 °C.

Fig. 6 plots the calculated marginal capacities of the positive and negative electrode, δ_p and δ_n. All dotted lines were the results of regression by power functions. As shown in Fig. 6, δ_n increased steeply, while δ_p, decreased moderately. To evaluate ΔLi_{loss} in accordance with Eq. (6), $q_p(t)$ and $q_n(t)$ must be evaluated as described in the last part of Section 3.2. Fig. 7a shows $q_p(t)$ change stored at 3.63 V under 25 °C or 60 °C, and Fig. 7b shows that for

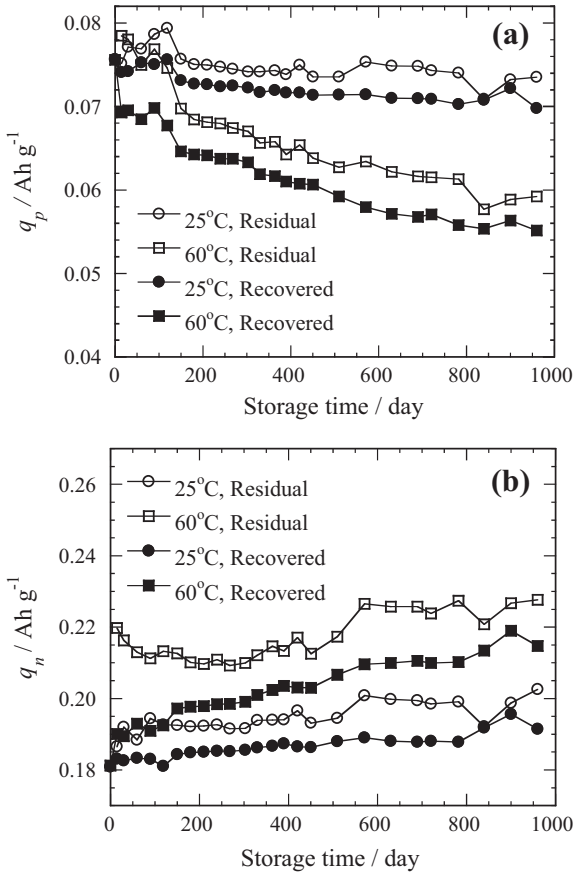

Fig. 7. Change of residual and recovered discharged capacities: (a) positive electrodes, and (b) negative electrodes.

$q_n(t)$. q_p and q_n of "residual" corresponded to the cell voltage, which were measured just after storage of prescribed days, lowered to less than 3.63 V by self discharge during storage. The horizontal axis for "residual" q_p or q_n shows the days when the previous storages ended and the cell voltages were measured. On the other hand, q_p and q_n of "recovered" meant that they corresponded to 3.63 V of the cell voltage set for the following storage. The horizontal axis for "recovered" q_p or q_n shows the days on which the cells were charged to 3.63 V and the following storages started. In accordance with the definition, "residual" and "recovered" discharged capacities do not mean the quantity of the cell capacities to be discharged, but they are a kind of q_p or q_n defined in Fig. 2. That is to say, they show the distance from the origin of horizontal axis in Fig. 2. Therefore, "residual" included both of reversible and irreversible self discharge capacity, while "recovered" did not include the reversible. This is the reason why "residual" was larger than "recovered".

Fig. 8 shows $Li_{loss}(t)$ calculated in accordance with Eq. (6) using $m_p(t)$, $m_n(t)$, $q_p(t)$, and $q_n(t)$ shown in Figs. 5 and 7, which is the accumulated irreversible capacity loss until certain storage time t. The dotted lines are fitting curves based on the $t^{1/2}$ rule. Good fitting of the curves in the almost all area in Fig. 8 indicates that $Li_{loss}(t)$ corresponds to the mass of lithium in the SEI film formed during the calendar life tests, because the $t^{1/2}$ rule was proposed by Peled assuming formation and growth of SEI [1]. The non-zero intersect appearing in Fig. 8 at 60 °C may imply that the SEI growth during the first storage term at 60 °C was exceptionally fast.

4.2. Capacity-fading prediction

All the results and discussion on the analysis of $dV_{cell}(Q)/dQ$ described above suggest that three indicators for the capacity fading of lithium-ion cells, m_p, m_n, and Li_{loss}, were the functions of the storage time. Therefore, $dV_{cell}(Q)/dQ$ at any storage time t can be reproduced in reverse from $m_p(t)$, $m_n(t)$, and $Li_{loss}(t)$. The capacities at any storage time t can also be calculated with $V_{cell}(Q)$ transformed from the reproduced $dV_{cell}(Q)/dQ$.

We demonstrated this idea by the following steps: (1) measure $dV_{cell}(Q)/dQ$ up to 360 days and analyze them into the functions of $m_p(t)$, $m_n(t)$, and $Li_{loss}(t)$; (2) construct $dV_{cell}(Q)/dQ$ up to 960 days from the functions; and (3) calculate capacities of the cells, $W_{cell}(t)$, up to 960 days and compare the calculated and measured capacities.

Examples of the first step have already been shown above: $m_p(t)$ and $m_n(t)$ decreased exponentially in accordance with Eq. (7), and $Li_{loss}(t)$ increased in accordance with the $t^{1/2}$ rule as shown in Fig. 8. In the second step, $dV_{cell}(Q)/dQ$ were constructed with Eqs. (2) and (4), which contains m_p, m_n, δ_p, and δ_n. Eq. (2) is transformed as

follows

$$\frac{d}{dt}(\delta_n - \delta_p) = \frac{d}{dt}(m_n q_n - m_p q_p)$$
$$= \left(m_n \frac{dq_n}{dt} - m_p \frac{dq_p}{dt}\right) + \left(q_n \frac{dm_n}{dt} - q_p \frac{dm_p}{dt}\right)$$
$$= \frac{dLi_{loss}}{dt} + \left(q_n \frac{dm_n}{dt} - q_p \frac{dm_p}{dt}\right). \quad (8)$$

The integral of Eq. (8) from t_1 to t_2, supposing fixed q_p and q_n as $\langle q_p \rangle$ and $\langle q_n \rangle$, will be

$$\Delta(\delta_n - \delta_p) \cong Li_{loss}(t_2) - Li_{loss}(t_1) + \langle q_n \rangle (m_n(t_2) - m_n(t_1)) - \langle q_p \rangle (m_p(t_2) - m_p(t_1)), \quad (9)$$

where $Li_{loss}(0)$ was assumed to be zero as the starting point.

The value of $(\delta_n - \delta_p)$ at a certain storage time is the sum of $\Delta(\delta_n - \delta_p)$ until the time and the initial value of $(\delta_n - \delta_p)$ determined by fitting the initial $dV_{cell}(Q)/dQ$. In constructing $dV_{cell}(Q)/dQ$, δ_p was temporarily regarded as zero. The initial $dV_{cell}(Q)/dQ$ was constructed with $m_p(0)$, $m_n(0)$, and the initial value of $(\delta_n - \delta_p)$ in accordance with Eqs. (2) and (4). Then, the discharge curve of the cells after 30 days was constructed as follows. First, $\langle q_p \rangle$ and $\langle q_n \rangle$ in Eq. (9) corresponding to the specific voltage of the cell from 0 to 30 days were derived from the constructed initial $dV_{cell}(Q)/dQ$ in the way described in Section 3.2. Secondly, $(\delta_n - \delta_p)$ after 30 days were calculated by adding $\Delta(\delta_n - \delta_p)$ in Eq. (9) to the initial value of $(\delta_n - \delta_p)$. Lastly, the discharge curve of the cells after 30 days was constructed with $m_p(30)$, $m_n(30)$, and $(\delta_n - \delta_p)$ after 30 days. Discharge curves of the cells beyond 30 days were constructed in the same way.

Fig. 9 compares the predicted and the measured differential discharge data stored for 960 days at 60 °C. The predicted differential discharge curves after 960 days were constructed with the calendar-life test data up to 360 days in the way explained above. On the other hand, the fitted ones were directly calculated with the measured $dV_{cell}(Q)/dQ$ after 960 day storage in the way shown in Section 3.1. Although the predicted and fitted positive discharge curves differed somewhat, the predicted discharge curve of the cell fitted the measured values very well. The difference between the predicted and the fitted came from the rather low accuracy of the usable mass of the positive active materials. Since the potential changes in positive electrodes were smaller than those in negative electrodes within the cell voltage window, the fitting results of the positive electrodes seemed to accompany greater error.

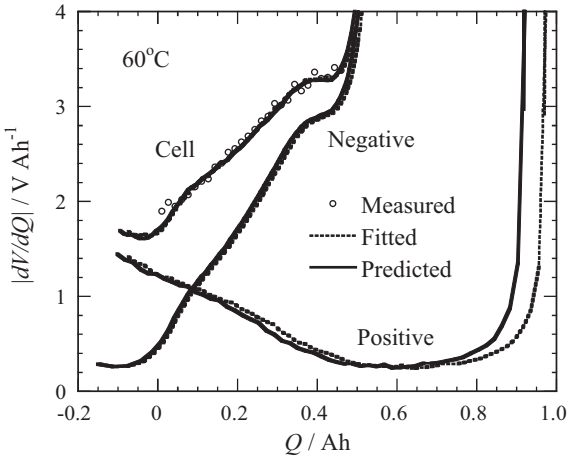

Fig. 9. Predicted discharge curves and measured discharge curves when lithium-ion cells were stored for 960 days at 3.63 V and at 60 °C.

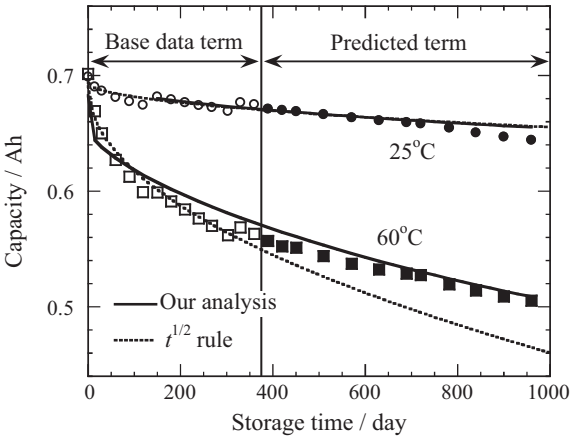

Fig. 10. Measured capacities (symbols) and the predicted by our analysis and by $t^{1/2}$ rule; capacities after 360 days were calculated on basis of test data before 360 days.

In the third step, the cell capacities were calculated using the predicted discharge curves of the cells and the cell voltage window prescribed as 4.09 V to 2.72 V for 25 °C and as 4.08 V to 2.73 V for 60 °C. Fig. 10 shows the predicted capacity curves with our analysis, that with the conventional $t^{1/2}$ rule, and the measured capacities. Solid lines are predicted capacities based on our analysis, while dotted lines are the predicted capacities based on the $t^{1/2}$ rule. Empty symbols are the capacities measured and used for the analysis, and the black ones are the capacities measured but not used for the analysis. All predicted capacities are calculated on the basis of the calendar life test data up to 360 days. As for the results for 25 °C, both the solid and dotted lines fit the symbols up to 960 days, which is consistent with the almost constant m_n shown in Fig. 5. Although m_p moderately decreased in this case as shown in Fig. 5, its effect on the cell capacities is limited because of the small potential change in the positive electrode. Therefore, the decreases in the cell capacities in this case mainly depend on increases in Li_{loss} expressed by the $t^{1/2}$ rule. On the other hand, for 60 °C, the dotted line based on the $t^{1/2}$ rule deviates from the symbols gradually after 300 days, while the solid line fits the symbols well on the whole. In this case, the decreases in m_p and m_n are large enough to be taken into account as shown in Fig. 5. Hence the cell capacities are determined by the complex interaction among decreasing m_p, decreasing m_n, and increasing Li_{loss}. Therefore, the conventional $t^{1/2}$ rule is too simple to cope with this complicated situation.

The new prediction method based on the discharge curve analysis was more accurate than the $t^{1/2}$ rule method when the predictions were based on the data from zero to 360 days. Whether this tendency stays the same even if the range of data used for the prediction is shortened or extended is a significant question. The answer is shown in Fig. 11. The horizontal axis shows the days during which the data for the analysis were measured. The vertical axis is the deviation ratio (%) to the measured capacity after 960 days, which is $[W_{pred}(t) - W_{meas}]/W_{meas}$, where $W_{pred}(t)$ is the predicted capacity after 960 days based on the data up to t days, and W_{meas} is the measured capacity after 960 days. As far as the 25 °C data are concerned, both our analysis and the $t^{1/2}$ rule could precisely predict the cell capacity measured after 960 days if they were based on the measured data up to 200 days or more. However, as for 60 °C, the $t^{1/2}$ rule could not predict the cell capacity well after 960 days even if the fitting range was extended to 840 days. These results explicitly show the superiority and validity of the technology we have developed.

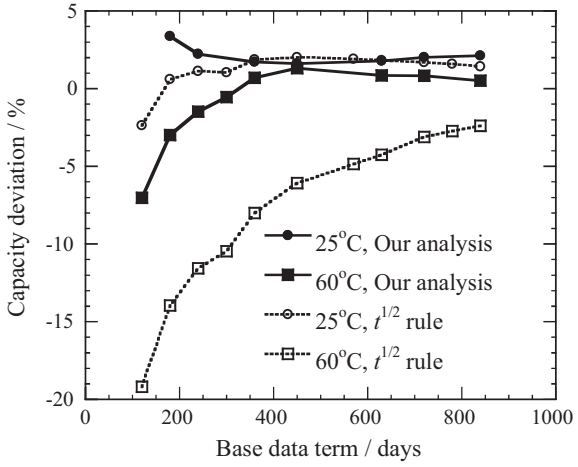

Fig. 11. Accuracy of capacity prediction by our analysis and $t^{1/2}$ rule; deviation of measured capacity after 960 days from predicted capacity as function of data accumulation term.

5. Conclusion

We have developed a new technology to predict the capacities of lithium-ion cells after storage at 25 °C and 60 °C using the analysis of discharge curves of the cells. Periodic measurement of the discharge curves of the lithium-ion cells during the calendar-life test and their analysis enabled us to derive the positive and negative discharge curves. The usable masses of the positive and negative active materials were analyzed by evaluating their discharge curves and were shown to decrease not following the $t^{1/2}$ rule but exponentially. The exponential changes of usable masses revealed to be much larger at 60 °C than that at 25 °C. The irreversible capacities of lithium ions derived from the analysis of discharge curves was determined to mostly follow the $t^{1/2}$ rule at both 25 °C and 60 °C. Consequently, the discharge curves of the cells at any storage time up to 960 days were definitely reproduced from the data up to 360 days, by adjusting three deterioration indicators: the positive usable mass, the negative usable mass, and the irreversible lithium loss. Our technology to predict the capacities up to 960 days from the data up to 360 days reproduced the measured capacities of cells both at 25 °C and 60 °C better than the conventional $t^{1/2}$ rule.

Although all the results of the analysis were hitherto consistent, we have to prove these results qualitatively and quantitatively by other analyses, such as disassembling the lithium-ion cells, in order to confirm the scheme formed by the analyses to be true. We applied our method to merely one-cell chemistry in this study. Therefore, one of our important future works will be to prove its availability for other cell chemistries in order to generalize the concept on which it is based.

List of symbols

$dV(Q)/dQ$	differential discharge curve
Li_{loss}	capacity of the irreversible lithium loss in the side reactions, Ah
m	usable mass of the active materials contributing discharge capacity, g
m_0	total mass of the active materials mounted on the electrode, g
q	discharged capacity per unit mass of active material to a certain point of discharge process, Ah g^{-1}
Q	discharged capacity for the lithium-ion cells, Ah
t	storage time, day
V	potential of the electrode, or cell voltage, V
V_{sp}	potential of the electrode per the unit mass of active material, V
$V(Q)$	discharge curve
w	full capacity of the electrode per the unit mass of active material, Ah g^{-1}
W	full capacity of the lithium-ion cells, Ah
α	utilization ratio of the active materials contributing to capacity at the initial state
β	coefficient of extent of the decreasing utilization ratio of the active materials
δ	marginal capacity of the electrode remained uncharged in fully charged state of the cells, Ah
τ	time constant of the fading process of active material mass, day

Subscript

p	positive electrode
n	negative electrode
cell	lithium-ion cell

References

[1] E. Peled, J. Electrochem. Soc. 126 (1979) 2047–2051.
[2] H.J. Ploehn, P. Ramadass, R.E. White, J. Electrochem. Soc. 151 (2004) 456–462.
[3] T. Yoshida, M. Takahashi, S. Morikawa, C. Ihara, H. Katsukawa, T. Shiratsuchi, J. Yamaki, J. Electrochem. Soc. 153 (2006) 576–582.
[4] M. Broussely, S. Herreyre, P. Biensan, P. Kasztejna, K. Nechev, R.J. Staniewicz, J. Power Sources 97–98 (2001) 13–21.
[5] P. Ramadass, B. Haran, R. White, B.N. Popov, J. Power Sources 112 (2002) 614–620.
[6] I. Bloom, A.N. Jansen, D.P. Abraham, K.L. Gering, J. Power Sources 139 (2005) 295–303.
[7] Q. Zhang, R.E. White, J. Power Sources 179 (2008) 785–792.
[8] A.J. Smith, J.C. Burns, J.R. Dahn, Electrochem. Solid-State Lett. 14 (2011) A39–A41.
[9] K. Honkura, H. Honbo, Y. Koishikawa, T. Horiba, ECS Trans. 13 (19) (2008) 61.